JOURNAL OF MATERIALS SCIENCE 11 (1976) 111–117

Tensile deformation behaviour of ABS polymers

R. W. TRUSS, G. A. CHADWICK
Department of Mining and Metallurgical Engineering, University of Queensland, St. Lucia, Queensland 4067, Australia

Several grades of ABS polymer have been tested in uniaxial tension over a temperature range from 293 K (20° C) to 198 K (−80° C). Effects of strain-rate and temperature on the yield stress have been explored and the magnitude of the activation volumes and activation energies derived. Additionally, the volume strain and the longitudinal strain have been monitored simultaneously, from which data the contribution of crazing to the total deformation of the specimens has been obtained.

1. Introduction

When tested in compression, polystyrene is known [1] to deform by the passage of narrow ($\simeq 1\,\mu m$ thick) shear bands through the specimen. The local deformation in these shear bands can be as high as 200% whilst the rest of the material remains relatively undeformed. When tested in compression [1] at high temperatures or low strain-rates, polystyrene deforms by the formation of diffuse shear zones which broaden and interact as the plastic strain is increased. The strain in these broad zones never exceeds by more than a few percent the strain in the rest of the unsheared matrix material. Evidence is available [2, 3] which indicates that similar bands develop under tensile loading conditions. When tested in tension polystyrene deforms by the formation of crazes perpendicular to the applied stress axis [4].

ABS, a two-phase material consisting of elastomer particles in a glassy polymer matrix similar to polystyrene, is also known to deform to some extent by crazing when tested in tension but the degree to which shear deformation may promote craze formation is not known. In this connection the following points are relevant:

(1) Bucknall and Smith [5] have suggested that the rubber particles can act as stress raisers allowing crazes to form in the glassy matrix phase at lower stresses than would otherwise be the case. This lowering of craze initiation stress was also observed by Wang *et al.* [6] in experiments with an embedded rubber sphere in polystyrene. They also performed experiments with two embedded spheres [7] and showed that, provided the distance between the spheres was sufficiently small, their stress fields would interact and increase the stress at the rubber–matrix interface, thus further reducing the applied stress required for craze initiation.

(2) Bucknall and co-workers [8–10] have shown that, by monitoring both the longitudinal and volume strains during creep, the relative contributions of shear deformation and crazing can be evaluated. It was shown that in HIPS the contribution of crazing to the total recorded deformation could approach 100%; for HIPS/PPO blends the contribution was in the region of only 30%; and for a certain commercial grade of ABS crazing was observed to become significant only after considerable initial shear deformation.

In the present work several grades of ABS, having different rubber contents and different matrix molecular weights, were tested in uniaxial tension. The effects of temperature and strain-rate on the deformation characteristics were studied in order to assess the applicability of the Eyring rate equation to the yield-point behaviour of these materials. The Eyring equation has been found to describe the yield stress variation with strain-rate and temperature for a number of glassy polymers [11, 12]. The equation is derived for a single, thermally activated process and is given by

© *1976 Chapman and Hall Ltd. Printed in Great Britain.*

$$\dot{\epsilon} = A \exp\left\{\frac{-(\Delta H - \sigma v)}{kT}\right\} \quad (1)$$

where $\dot{\epsilon}$ is the stain-rate, σ the applied stress, v the activation volume, T the absolute temperature, k Boltzmann's constant and A a constant. ΔH is the activation energy for the process. Equation 1 rearranges to

$$\frac{\sigma_y}{T} = \frac{\Delta H}{vT} + \frac{k}{v}\ln\left(\frac{\dot{\epsilon}}{A}\right) \quad (2)$$

indicating that plots of σ_y/T versus $\dot{\epsilon}$ for various temperatures should give a family of parallel straight lines provided that ΔH and v are constant. From such an analysis of the data obtained on ABS it was hoped to gain information concerning the operative deformation process at yield.

Tests were also conducted such that the longitudinal strain and volume strain could be measured simultaneously to determine the deformation regime over which crazing was an important deformation mechanism.

2. Experimental

2.1. Materials

The materials used were various grades of Cycolac brand commercial ABS with varying rubber content and matrix molecular weight. These materials had a constant average rubber particle size and were designated as shown in Table I.

TABLE I Designation of materials used

Rubber content	Molecular weight	
Low	low	high
Low	A	
Medium	B	D
High	C	E

The bars for room temperature tensile tests were injection moulded to a shape specified by B.S. 2782 having a parallel gauge length of 50.8 mm with a cross-section 12.7 mm by 3.2 mm. Test pieces of materials B and D for low temperature tests were milled from 3.2 mm sheet with a 37 mm parallel gauge length and a gauge width of 7 mm. All specimens were annealed at approximately 80° C for 2 h before testing.

2.2. Tensile tests

Room temperature tests were conducted on materials with varying rubber content over a range of strain-rates to determine the effect of rubber content and strain-rate on the yield stress. Material B was tested over a range of temperatures and strain-rates to determine whether or not these materials obey the Eyring equation. The low temperature range of −80° C to room temperature was chosen so that the variation of yield stress with temperature could also be obtained in the region of the glass transition of the rubber. The higher molecular weight material D was also tested at room temperature and −30° C to investigate the effect of molecular weight of the matrix on the yield stress and the parameters of the Eyring equation.

Room temperature tests were conducted on an Instron testing machine at constant cross-head speeds ranging from 0.5 to 500 mm min^{-1}. The machine was considered hard with respect to the specimen and strain-rates were calculated from the cross-head speed. This gave strain-rates of approximately 10^{-4} to 10^{-1} sec^{-1}. Low temperature tests were conducted on a tensile machine fitted with a cryostat: test specimens were enclosed in a vacuum flask, low temperatures being achieved by the controlled boil off of liquid nitrogen. The cross-head speeds used on this machine ranged from 0.5 to 22 mm min^{-1} which gave a strain-rate range of 2.5×10^{-4} to 10^{-2} sec^{-1}.

2.3. Volume strain measurements

The contributions of crazing and shear deformation to the longitudinal strain were calculated by measuring volume strain during a tensile test and thus obtaining plots of volume strain versus longitudinal strain similar to those of Bucknall and Clayton [8]. The volume strain was obtained by a displacement method, the specimens being tested in a constant volume perspex container filled with water. The container was connected to a capillary so that any volume change in the specimen could be calculated from the height of the column of water in the capillary. At high strain-rates, the duration of the test was only a few seconds and the rate of fall of the meniscus in the capillary was extremely rapid. In these cases, the meniscus was monitored using a high speed camera taking a constant number of frames per second. The meniscus level was then measured from the film.

3. Results

3.1. General observations

A typical load–extension curve obtained for these ABS materials is given in Fig. 1. A distinct yield point was observed where the specimens extended

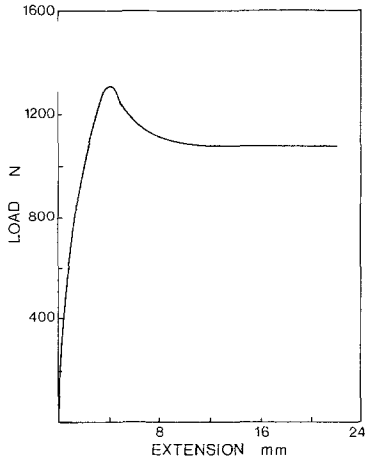

Figure 1 Load–extension curve for Cycolac C at strain-rate 2.78×10^{-4} sec^{-1}.

without a further increase in the applied load. It was at or near this yield point that, at low strain-rates, diffuse shear zones appeared on the edges of the test piece and began to propagate obliquely into it. These areas of local strain produced a small indentation on the surface. They were also highly stress whitened. During the load drop following the yielding of the material, these shear zones appeared over the whole gauge length and began to propagate slowly into the specimen, broadening from the point of initiation. This gave a wrinkled appearance to the surface. At high strain-rates, no distinct shear zones were observed but the yield point was associated with a general clouding of the whole gauge length. The specimens tested at low temperatures could not be observed during the test but the general appearance of the test piece after fracture was similar to that of the high strain-rate tests with a general whitening over the whole gauge length. Fig. 2 illustrates shear band and craze formation in specimens tested to fracture at four different strain-rates.

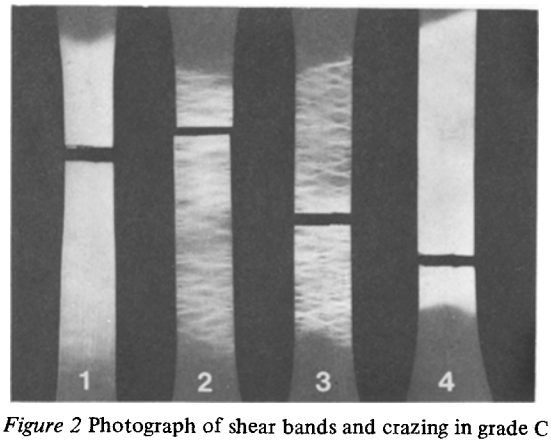

Figure 2 Photograph of shear bands and crazing in grade C ABS tested at room temperature at four different strain-rates: 1. 1.39×10^{-4}, 2. 1.39×10^{-3}, 3. 1.39×10^{-2} and 4. 1.39×10^{-1} sec^{-1}.

The period of extension of the specimen at constant or slightly decreasing load was accompanied by continued stress whitening of the gauge length. Fracture finally occurred in a highly stress whitened region of the gauge length. Cracks were observed to propagate slowly at first but rapidly when the reduced cross sectional area could no longer support the increased stress. Fracture was perpendicular to the applied stress on all occasions even when pronounced oblique shear zones were present. On some occasions irregular steps appeared on the fracture surface due to the linking up of cracks propagating on different planes.

3.2. Yield point measurements

Fig. 3 shows a plot of σ_y/T versus log $\dot{\epsilon}$ for material B for various temperatures; a family of parallel straight lines was obtained fitting Equation 2 quite well. From measurements of the average slope of the lines and their y intercepts, the parameters of Equation 2 were calculated as $v = 2300$ Å^3, $\Delta H = 39.2$ kcal mol^{-1}. A similar plot to Fig. 3 was obtained from yield point measurements on the higher molecular weight material D. Here, the thermodynamic parameters were found to be higher than those obtained for material B, namely

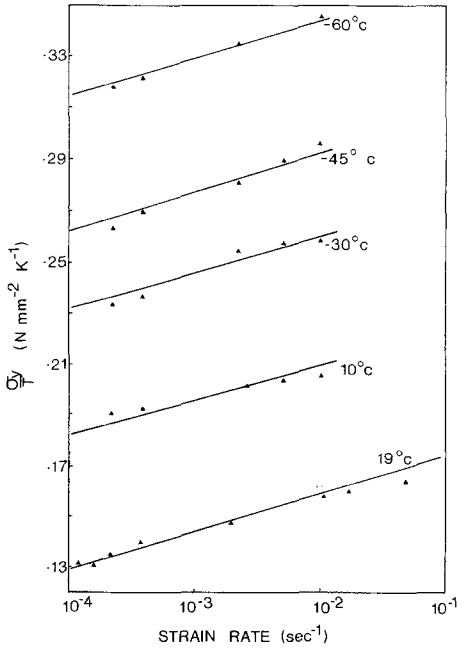

Figure 3 σ_y/T versus strain-rate for material B at various temperatures.

$v = 3175\,Å^3$. $\Delta H = 61.5\,kcal\,mol^{-1}$.

Activation volumes were also obtained from room temperature tensile tests for the other grades of ABS material available and the complete set of results is listed in Table II. It can be seen that there is a marked difference in activation volume between the grades of ABS having different matrix molecular weights, the higher molecular weight material having the higher activation volume. Also evident is a slight tendency for an increase in activation volume with increasing rubber content for ABS having a constant matrix molecular weight,

TABLE II Room temperature activation volumes for different grades of ABS

ABS grade	Activation volumes ($Å^3$)
Low mol wt	
A	2500
B	2500
C	2700
High mol wt	
D	3300
E	3700

although these small changes in values are actually within the experimental error ($\pm \simeq 10\%$). This apparent trend is consistent with a model in which the rubber particles act as stress raisers and in which, for the higher rubber content materials, the stress fields of adjacent rubber particles interact.

In materials having a constant matrix molecular weight, the yield strength at constant strain-rate increased with decreasing rubber content, from

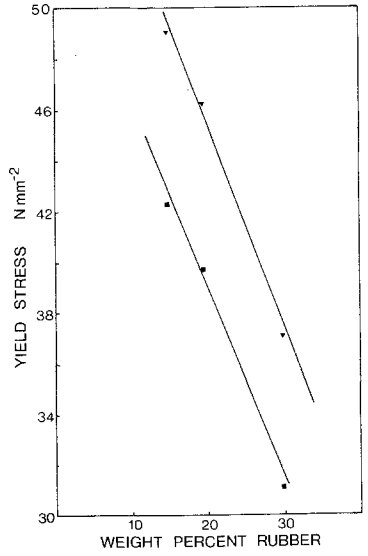

Figure 4 Yield stress as a function of the rubber content for the materials with a low molecular weight matrix: (■) $1.39 \times 10^{-4}\,sec^{-1}$, (▼) $1.39 \times 10^{-2}\,sec^{-1}$.

31.3 and 37.1 $N\,mm^{-2}$ for the high rubber content material C at strain-rates 1.39×10^{-4} and $1.39 \times 10^{-2}\,sec^{-1}$ respectively to 42.3 and 49.2 $N\,mm^{-2}$ for the low rubber content material A at the above strain-rates. This trend is shown in Fig. 4.

It follows from Equation 2 that the relationship between yield stress at constant strain-rate and temperature should be linear and this trend was in fact observed in the temperature range used in these experiments. However, at all but the lowest strain rate used, brittle failure occurred at $-80°$ C before yielding.

3.3. Volume change measurements

It was found that, within experiment error, the volume of the test specimen was constant until yield, at which point the volume increased quite rapidly with the simultaneous onset of stress whitening in the specimen. This rapid increase in the volume strain was found to continue during the drop in load on the specimen. During the period of extension at relatively constant load, a lower but still constant rate of volume increase was recorded.

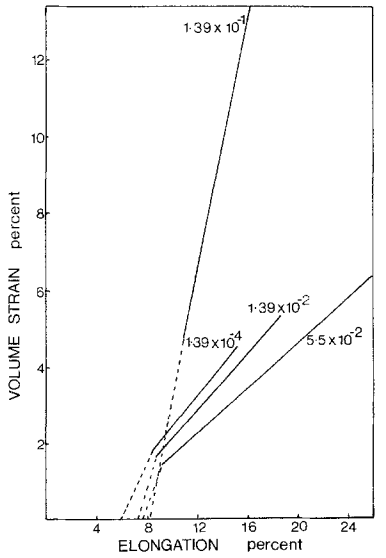

Figure 5 Volume strain versus longitudinal strain for material B tested at room temperature at varying strain-rates. Curves for other materials have similar slopes.

Fig. 5 shows plots of volume strain ($\Delta V/V\%$) against longitudinal strain ($\Delta L/L\%$) for a range of strain-rates. It was found that the slope of these lines during the period of extension at approximately constant load was relatively independent of rubber content but varied with the strain-rate. The slopes of the lines at given strain-rates are given in Table III. The initial part of the plot was not

TABLE III Contribution of crazing to the deformation at various strain-rates

Strain-rate (sec^{-1})	Slope of line in Fig. 4	Contribution of crazing (%)
1.39×10^{-4}	0.446	44.6
1.39×10^{-2}	0.386	38.6
5.5×10^{-2}	0.287	28.7
1.39×10^{-1}	1.000	100

always linear but in general the initial rate of volume increase was higher than at later stages of the deformation. Following the arguments and procedure of Bucknall and Clayton [8], the contribution of crazing to deformation has been computed and these figures are also shown in Table III.

For the lowest three strain-rates, the contribution of crazing decreases with increasing strain-rate, yet at the highest strain-rate used the contribution of crazing rises sharply to 100%.

4. Discussion

4.1. Yield stress behaviour

The experimental data obtained fit the Eyring viscosity equation for a single deformation process in the ranges of temperature and strain-rate used. Although Equation 1 was developed to account for viscoelastic deformation, it could equally well apply to other thermally activated processes such as crazing. The activation parameters of Equation 2 were found to exhibit a strong variation with the matrix molecular weight but were practically independent of rubber content, indicating that the yield point phenomena were controlled more by the macromolecular structure of the matrix than by the distribution of rubber particles.

From the general observations of the deformation process, such as shear band formation and the associated stress whitening, and also from the volume strain measurements, it is clear that both yielding of the matrix and crazing are occurring at or near the yield point. The derived values of activation energy and activation volume for ABS are not inconsistent with reported values of these parameters obtained from shear deformation studies on other glassy polymers [10–12]. It is possible, however, that activation volumes and energies for crazing would be of similar magnitude to those for shear deformation, but such data on crazing are not readily available. It is not possible, therefore, with the present experimental results to determine which of the two processes governs the yielding of ABS materials. Further experiments are currently in progress on clear ABS to attempt to establish unequivocally the mechanisms involved in the yield and post-yield deformation of these two-phase materials.

Irrespective of the mechanism of yielding, an important aspect of these results is the fact that increasing the rubber content decreases the yield stress (Fig. 4). There are several means by which the addition of discrete rubber particles to the glassy SAN matrix could influence the yield stress. First, there is a simple statistical effect in which the load bearing volume of the matrix is decreased. If this reduction in load bearing volume were the only effect of the addition of rubber particles, a normalized yield stress calculated on the cross-sectional area of the matrix supporting the load would be expected to be constant. Such is not the case since a marked drop in the normalized yield stress occurs in the high rubber content material as shown in Fig. 6. Thus the decrease in load carrying volume of the matrix cannot account entirely for the change in yield stress with increasing rubber content.

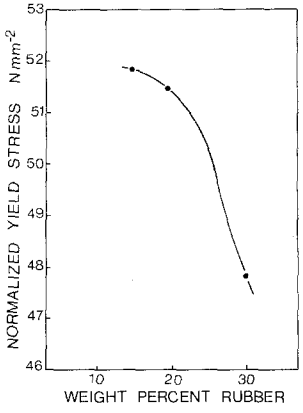

Figure 6 Normalized yield stress as a function of rubber content for the low molecular weight materials.

A second possible interpretation is that, since the rubber particles have a different modulus from the matrix, they act as stress raisers and points of inhomogeneity in the strain field. They should thus promote viscous flow and the formation of shear zones at lower applied stresses. Matsuo *et al.* [7] have shown that the distance between two rubber balls must be below a critical value before significant interaction of their stress fields will take place. They found that this critical spacing was approximately given by

$$\frac{l}{d} = 1.45$$

where l is the centre-to-centre distance between the two rubber balls and d is the diameter of the balls. Although the experiments of Matsuo *et al.* were conducted on the very simple case of two rubber balls embedded in polystyrene, their results correlate quite well with the results obtained for the more complicated ABS system, as can be seen from the following calculations.

To obtain an estimate of the planar separation of the rubber particles in the ABS materials, the square lattice spacing (l') was used [13]. This is given by

$$l' = \left[\left(\frac{\pi}{f}\right)^{\frac{1}{2}} - 2\right] r_s$$

where f is the volume fraction of the rubber particles and r_s is the average radius of circular sections of the rubber particles on an intersecting plane given by

$$r_s = \left(\frac{2}{3}\right)^{\frac{1}{2}} r$$

where r is the average radius of the particles. Thus

$$\frac{l}{d} = \frac{l' + 2r_s}{2r_s}.$$

This gave values for the various rubber contents as shown in Table IV.

TABLE IV l/d values for low, medium and high rubber content materials

Material	Rubber content	l/d
A	low	2.15
B	medium	1.85
C	high	1.29

The values of l/d for the two lower rubber content materials, A and B are larger than the critical value of 1.45 given by Matsuo *et al.* and above which interaction between particles is negligible. It would be expected that the interaction of the stress fields of the rubber particles in these two materials would be small and thus little change in the normalized yield stress would be expected. On the other hand, the highest rubber content material gave an l/d ratio of 1.29. Thus, the much smaller distances between the particles of this material could initiate yield at lower applied stress levels due to the creation of regions of high interacting stress fields.

It would be expected that this stress concentration effect would be reduced at temperatures below the glass transition temperature of the rubber particles ($\simeq -75°$ C) since at these temperatures the glassy rubber particles would have a modulus similar to that of the glassy matrix. However, at a strain-rate of $2.5 \times 10^{-4}\text{sec}^{-1}$, a linear relationship between yield stress and temperature is maintained down to $-80°$ C for the medium rubber content material. Higher strain-rates at $-80°$ C produced brittle failure before measureable yielding occurred. Brittle failure presumably occurs because the glassy rubber particles cannot act as efficient craze terminators, thus allowing large crazes to develop in which cracks can nucleate and propagate.

4.2. Volume strain measurements

The volume strain measurements indicate that the yield point is associated with the onset of crazing in the material. The rate of crazing is initially higher than the constant rate recorded after the post-yield drop in load. For strain-rates 1.39×10^{-1} and $5.5 \times 10^{-2}\text{sec}^{-1}$ crazing can account for all of the longitudinal strain being produced in the specimen during the load drop but for lower strain-rates, the contribution of crazing to the deformation during the load drop is less than 75%. By way of contrast, in all specimens except those tested at the highest strain-rate, a significantly greater amount (up to 70%) of shear deformation and other non-cavitational processes contributes to the deformation during the steady deformation period after the load drop.

Specimens deformed at a strain-rate of $1.39 \times 10^{-1}\text{sec}^{-1}$ showed anomalous behaviour. At this strain-rate, the slope of the line of the volume strain versus longitudinal strain was slightly greater than unity. This unexpected result is possible due to the introduction of a large reserve of elastic energy in the system followed by the release of this energy in craze formation. This phenomenon could be amplified by the method of measuring volume changes in the present experiments: any hysteresis in the response of the water reservoir would tend to increase the slope of the volume strain versus longitudinal strain line, an effect that would be most serious at the highest strain-rates.

Crazing initiates at the yield point and, therefore, the Eyring analysis of the yield point data could, in fact, relate to craze initiation rather than shear deformation processes. However, in the absence of other data on the activation energies and activation volumes for craze initiation from

other glassy polymers with which to compare the the values obtained in this work, such an interpretation must remain entirely speculative.

5. Conclusions

(1) The several grades of ABS examined obey the Eyring viscosity equation, suggesting that a single flow process is operating in the strain-rate range 10^{-4} to $10^{-1}\,sec^{-1}$ between -60 and 20° C. The Eyring activation volume and activation energy calculated from the yield point data increase with an increase in molecular weight of the matrix. As crazing was shown to occur at the yield point, the computed thermodynamic parameters could possibly relate to craze initiation.

(2) The yield stress increases linearly with decreasing temperature between -80 and 20° C. An approximately linear increase in the yield stress accompanies a decrease in the rubber content in the range of 15 to 30 wt% rubber.

(3) The yield drop was associated with an initially high rate of crazing which decreased to a lower constant rate determined by the strain-rate for the period of extension at constant load. The constant rate appeared to be relatively independent of rubber content.

(4) An analysis of the yield stress data of a given grade of ABS with varying rubber contents was shown to be consistent with the idea that the rubber particles act as stress raisers for crazing. The data did not show any trend to support a critical strain requirement for crazing.

(5) At a strain-rate of $1.39 \times 10^{-1}\,sec^{-1}$, all the deformation was associated with crazing, while at lower strain-rates only approximately 25 to 50% could be attributed to crazing. The contribution of crazing increased with decreasing strain-rate in this low strain-rate region.

Acknowledgements

The polymeric material on which this research has been conducted was generously provided by Marbon Chemical (Australia) Pty Ltd. RWT is grateful for the provision of a Commonwealth University Scholarship.

References

1. P. B. BOWDEN and S. RAHA, *Phil. Mag.* **22** (1970) 463.
2. F. J. MCGARRY, *Proc. Roy. Soc.* A319 (1970) 59.
3. C. B. BUCKNALL, I. C. DRINKWATER, and W. E. KEAST, *Polymer* **13** (1972) 115.
4. R. P. KAMBOUR, *Macromol. Revs.* 7 (1973) 1.
5. C. B. BUCKNALL and R. R. SMITH, *Polymer* **6** (1965) 437.
6. T. T. WANG, M. MATSUO and T. K. KWEI, *J. Appl. Phys.* **42** (1971) 4188.
7. M. MATSUO, T. T. WANG and T. K. KWEI, *J. Polymer Sci. A-2* **10** (1972) 1085.
8. C. B. BUCKNALL and D. CLAYTON, *J. Mat. Sci.* 7 (1972) 202.
9. C. B. BUCKNALL, D. CLAYTON and W. E. KEAST, *ibid* 7 (1972) 1443.
10. C. B. BUCKNALL and I. C. DRINKWATER, *ibid* 8 (1973) 1800.
11. J. A. ROETLING, *Polymer* **6** (1965) 311.
12. C. BAUWENS-CROWET, J. C. BAUWENS and G. HOMÈS, *J. Polymer Sci. A-2* 7 (1969) 735.
13. L. M. BROWN and R. K. HAM, in "Strengthening Methods in Crystals", edited by A. Kelly and R. B. Nicholson (Elsevier, London, 1971) p. 34..

Received 7 April and accepted 11 June 1975